

für sich homogene Ketten, die in Richtung der Raumdiagonalen verlaufen; in aufeinanderfolgenden Ebenen wechseln die Ketten ihre Richtung. In Fig. 2 ist eine Zelle in flächenzentrierter Aufstellung gezeichnet, in die die kleinste Zelle (innenzentrierte Aufstellung, siehe Fig. 3) hineingestellt ist. Der Abstand zwischen zwei Kupferionen und zwischen zwei  $\text{N}_1$  beträgt jeweils 3,36 Å. (weitere Abstandsverhältnisse Tabelle 2).

Tabelle 2. Nachbarschaften des  $\text{CuN}_3$ -Gitters

Atomart	gleichw. Nachb.		Abstand in Å.
	Anzahl	Art	
Cu	4	Cu	3,36
	2	Cu	4,33
	2	Cu	5,15
	2	$\text{N}_1$	2,795
	4	$\text{N}_1$	3,36
	4	$\text{N}_{11}$	2,23
	2	$\text{N}_{11}$	3,28
	2	$\text{N}_{11}$	3,56
$\text{N}_1$	2	$\text{N}_{11}$	3,56

Alle anderen Nachbarschaften wie Cu

Das Gitter konnte, auch wenn nur der Schwerpunkt der  $\text{N}_3$ -Gruppe berücksichtigt wurde, nicht auf einen bekannten Gittertyp zurückgeführt werden.

Ein Vergleich der gefundenen Struktur mit den Azidstrukturen benachbarter Elemente in der ersten Gruppe des periodischen Systems zeigt, dass das  $\text{CuN}_3$  aus dem bisher beobachteten Bauprinzip herausfällt.

$\text{KN}_3$  kristallisiert in der Raumgruppe  $D_{4h}^{18}-I4/mcm$  und kann als ein deformiertes CsCl-Gitter aufgefasst werden (Hendricks & Pauling, 1925). Auch  $\text{AgN}_3$  gehört dem  $F5_2$ -Typ an, ist jedoch rhombisch und nur noch pseudotetragonal (Bassière, 1935). Die Zelle enthält in beiden Fällen 4 Moleküle. Beim  $\text{CuN}_3$  besteht die Zelle aus 8 Molekülen, und ein charakteristisches Merkmal der anderen aufgeführten Strukturen—zur Basis parallele, senkrecht aufeinanderstehende  $\text{N}_2$ -Ketten—ist nicht mehr vorhanden. Diese Anordnung ist nur noch in der Projektion auf die Basisebene wiederzufinden, gegen die die Ketten eine Neigung von  $36^\circ 43'$  haben. Die unerwartete Gitterbildung des Kupferions ist auch bei einigen anderen Cu-Verbindungen zu beobachten, z. B. beim Oxyd und den Halogenverbindungen.

Herrn Professor Dr. Masing danke ich für sein förderndes Interesse an dieser Arbeit, Herrn Professor Dr. Ernst für seine stetige Unterstützung.

### Schrifttum

- BASSIÈRE, M. (1935). *C.R. Acad. Sci., Paris*, **201**, 735.  
 HENDRICKS, S. B. & PAULING, L. (1925). *J. Amer. Chem. Soc.* **47**, 2904.  
 MARTIN, F. (1915). *Über Azide und Fulminate und das Wesen der Initialzündung*. Darmstadt.  
 STRAUMANIS, M. & CIRULIS, A. (1943). *Z. anorg. Chem.* **251**, 315.  
 WÖHLER, L. & KRUPKO, W. (1913). *Ber. deutsch. chem. Ges.* **46**, 2045.

*Acta Cryst.* (1948). **1**, 118

## The Use of the 'Fly's Eye' Apparatus to Study Crystal Structures containing Atoms of Different Scattering Powers

BY PIETER J. G. DE VOS\*

*Crystallographic Laboratory, Cavendish Laboratory, Cambridge, England*

(Received 28 January 1948)

### Introduction

The 'Fly's Eye' apparatus (Bragg, 1944), as improved by Stokes (1946), consists of a regular array of tiny perspex lenses embossed on a perspex sheet. Its purpose is to form a multiple photograph of a proposed crystal structure projected along some crystallographic direction. This multiple photograph can then be used as a diffraction grating for visible light, and it will give orders of diffraction which have intensities similar to the X-ray reflexions from the real crystal in a zone corresponding to the direction of projection.

A fly's eye apparatus is a valuable aid in the trial and error method of crystal analysis. It was, for example, extensively used by Bunn in the determination of the structure of penicillin.

\* Now at University of Stellenbosch, South Africa.

Originally the fly's eye consisted of an array of multiple pinholes instead of lenses, and the complete picture was obtained by moving a lamp into the different atomic positions, and exposing a photographic plate at every position of the lamp. A positive print of this negative photograph was then used as the diffraction grating. When the lens fly's eye was introduced it became practicable to use black disks on an illuminated background which gave the whole multiple picture at one exposure. This picture, consisting of transparent apertures on an opaque background, can be used at once as the optical diffraction grating. As this picture is remarkably clear and well resolved it becomes worth while to inquire fully into the relation between the number and intensity of the orders observed and the size and shape of the apertures.

### Theory of the grating

A lens is placed behind the grating and parallel monochromatic light is transmitted through it. The diffraction pattern which is observed in the focal plane of the lens is therefore the Fraunhofer diffraction produced by an array of circular apertures which repeat regularly in two dimensions on a square net. Consequently the pattern consists of an array of orders also arranged on a square net. The intensities of the different orders depend on the structure of the repeating pattern of apertures, but are also modulated by the single-aperture diffraction pattern produced by each of the circular apertures.

The angular spread of light behind the grating depends on the size of the apertures, i.e. on the size of the black disks used on the illuminated screen. The first minimum of the single aperture Fraunhofer diffraction pattern produced by each of the circular apertures occurs at an angle  $\theta$  such that

$$\theta = 1.22\lambda/d,$$

where  $d$  is the diameter of the circular aperture.

The number of orders of diffraction contained within this angular spread depends on the repeat distance of the grating. The angular separation of consecutive orders is given by

$$\sin \phi = \lambda/b$$

or

$$\phi = \lambda/b,$$

since  $b$ , the repeat distance, is much greater than  $\lambda$ .

If it is desired to observe  $n$  orders, these  $n$  orders must subtend an angle less than  $\theta$ , or

$$n\phi = n\lambda/b < 1.22\lambda/d,$$

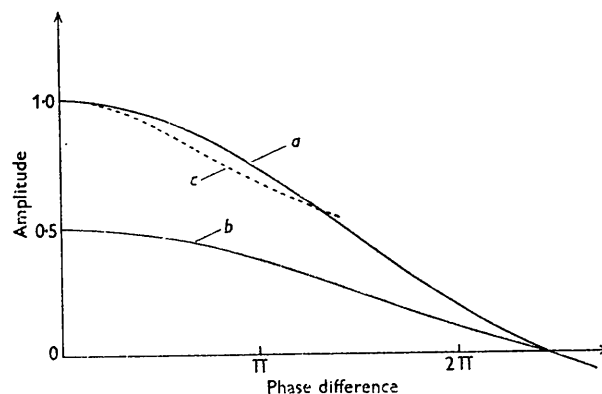
i.e. the ratio  $d/b$  should be less than  $1.22/n$ .

Clearly the ratio  $d/b$  is the same as the ratio between the diameter of the black disks and the side of the illuminated screen, which was 20 cm. in the apparatus used. To observe  $n$  orders therefore the diameter of the black disks had to be less than  $(1.22 \times 20)/n$  cm.

Consider first a structure containing one kind of atom only. It can be represented by a grating with apertures all of the same size. The intensity of the light at any point in the focal plane where the Fraunhofer diffraction pattern is observed is proportional to the square of the amplitude of the disturbance at that point. The intensity of reflexion of X-rays from a set of planes in an ideally imperfect crystal is proportional to the square of the scattering factor,  $f$ , of the atoms. In order that the corresponding orders of diffraction of visible light by the grating and of X-rays by the crystal should have the same intensities, it is apparent that the amplitude curve of the single aperture diffraction pattern and the  $f$ -curve of the atom it represents should be similar in shape.

Text-fig. 1 shows the amplitude curve of the central maximum of a circular single aperture. This curve has been drawn from tables given by Airy (1834), who was

the first to obtain a mathematical expression for it (see also Preston (1928), p. 324). Comparing it with a typical scattering-factor curve of an atom it is clear that it falls off rather too slowly near the origin, and too rapidly when it approaches the first zero value. Nevertheless, the size of the disks can be so chosen that the amplitude curve shows a fair amount of resemblance over a limited range to the atomic  $f$ -curve. The amplitude curve is plotted with an arbitrary scale of ordinates so chosen that it coincides with the  $f$ -curve at the origin. Its rate of falling off with angle, and therefore its position of intersection with the  $f$ -curve, depends on the radius of the disk. This is now so chosen that the intersection occurs at a certain angle  $\alpha$ , where all the orders being investigated (say the first five) lie within  $\alpha$  of the origin. If  $\alpha$  is still a fair amount smaller than the angle for the first zero value, the amplitude curve gives a satisfactory approximation to the  $f$ -curve over this



Text-fig. 1. Amplitude curve of single-aperture diffraction pattern against phase difference of light from opposite edges. *a*, Circular aperture; *b*, ring-shaped aperture of half area; *c*, scattering factor curve of silicon.

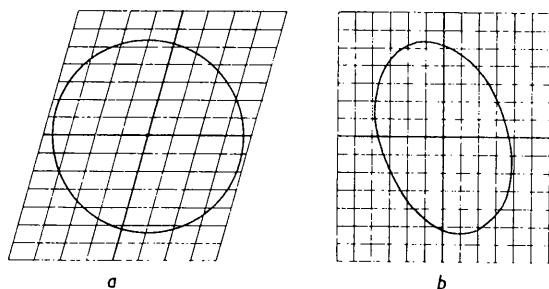
angular range. The consecutive orders of diffraction consequently show a satisfactory falling off in intensity in the same range. The dotted curve of Fig. 1 is an actual example. It shows how the  $f$ -curve for silicon could be made to fit approximately the amplitude curve of a disk. In the actual mineral in which these silicon atoms occurred, five X-ray orders fell within this angular range.

If the projected unit cell of the crystal is not approximately square, the diminution of  $f$  with X-ray orders is not the same in the two axial directions. It is obviously impractical to make a separate fly's eye apparatus with repeat distances between the lenses proportional to the axial lengths of the projected cell for every new crystal studied, nor is it necessary. The circular disks used need only be replaced by other shapes that give amplitude curves falling off at different rates along the axes. In his historic paper, Airy showed that the diffraction pattern of an elliptical aperture is also elliptical in shape with major and minor axes in the same ratio as those of the aperture, but transposed. If

therefore the unit cell is rectangular, the disks should be replaced by ellipses with major and minor axes proportional to the axial lengths, and they should be oriented on the square cell with their major axes coinciding with that edge of the fly's eye cell which corresponds to the short edge of the real cell.

When the unit cell is not rectangular, the shape and orientation of the ellipses that must be used can best be found by the following graphical method:

The reciprocal lattice net of the crystal projection is drawn and a circle described on it with centre at the origin and any radius fairly large compared with the axial repeat distances. All orders on this circle have the same Bragg angle  $\theta$ , and hence the same  $f$ . The points obtained by reading off the co-ordinates of the circumference on the reciprocal lattice net are now plotted on ordinary squared paper. This gives an ellipse. The squared paper may be considered to represent the reciprocal lattice of a square cell, and the ellipse on it now defines all orders which should have



Text-fig. 2. Graphical determination of the shape and orientation of the elliptical disks. *a*, Circular disk for non-rectangular cell; *b*, corresponding elliptical disk for square cell.

the same  $f$  if the real crystal cell is to be represented by a square fly's eye cell. If this ellipse is now turned through  $90^\circ$ , its shape and orientation gives the shape and orientation of the ellipses which should be used instead of circles on the illuminated background (Text-fig. 2).

#### Atoms of different scattering power

If the crystal structure is built up of atoms of different scattering power, either the disks representing the atoms should be made of different sizes or the opacity of their multiple images should be varied. The latter may be done by removing those disks representing the lighter atoms at appropriate times during the exposure which produces the multiple photograph. The objection to this is that it demands a very rigorously standardized development technique to ensure reproducible results, especially since high contrast photographic plates must be used.

The other alternative is to vary the area of the disks. The amplitude at the centre of the optical single-aperture diffraction pattern is proportional to the area of the aperture, and if a number of apertures of different sizes are used each gives an amplitude at the centre

proportional to its own area. The total amplitude there is then the sum of these constituents, since they are all in phase. The intensity at this point is therefore proportional to the square of the sum of the areas. Similarly the intensity of the zero-order X-ray reflexion is proportional to the square of the sum of the  $f$ -values. The area of each disk should therefore be made proportional to the  $f$ -value at  $\theta=0$  of the atom it represents.

The most obvious way of altering the area of the black disk is by altering its radius. However, the radius has already been fixed to satisfy the requirement that the amplitude curve shall be of the correct shape; it cannot now be altered to let the curve have the correct peak magnitude. Neither is there any possibility of a compromise, since the two requirements work in opposite directions: the amplitude curve of an aperture falls off more slowly the smaller the aperture, and the  $f$ -curve for an atom falls off more rapidly the lower the scattering power. The only other possibility is to cut out a hole from the centre of the disk. This has the result, as Airy has shown, that the diffraction pattern falls away faster and reaches its first minimum at a smaller angle than that of a solid disk.

Theory shows that the amplitude curve produced by such an annular aperture can be obtained by subtracting the amplitude curve of a circular aperture with radius equal to that of the central opaque patch from that of an aperture with radius equal to the outer radius of the annulus. This also follows at once from the consideration that the amplitudes at every point in the central maximum have the same phase, that is the phase that would be produced by a disturbance arising from an infinitely small element at the centre of the aperture.

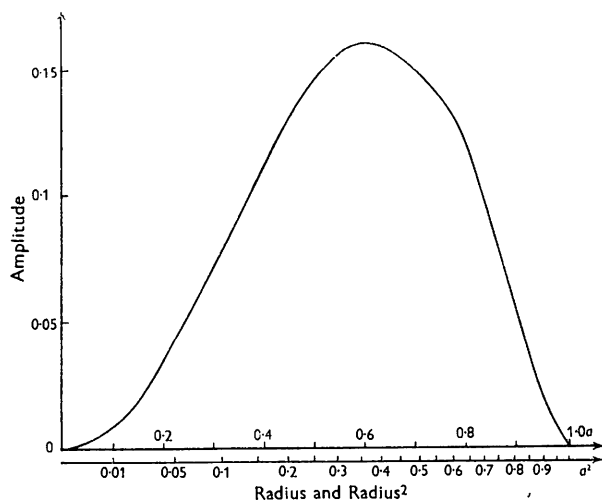
The correct procedure, therefore, to reduce the area of the aperture without altering the angular spread of its diffraction pattern is to make a central hole in the black disk (which contracts the angular size of its eventual diffraction pattern) and also to reduce its outside radius (which expands the pattern again to its original angular extent). For every area wanted there exists a pair of radii defining an annular aperture which will give a diffraction with central maximum of the same angular extent as the central maximum of the largest circular aperture employed in a given fly's eye picture (i.e. that satisfying the requirements of the preceding section).

The secondary maxima produced by such ring-shaped apertures are much more pronounced than those of circular apertures, but these do not concern us here.

Text-fig. 3 shows a graph from which these pairs of radii can be read off at once. It is really a plot of the calculated amplitude produced by a circular aperture of any radius  $a$ , where  $a$  is a fraction, in that angular direction in which the amplitude curve of an aperture of unit radius would fall to its first zero value. A straight-edge laid across the graph parallel to the  $a$ -axis fixes two fractional radii,  $a_1$  and  $a_2$ , which both produce the same amplitude in the angular direction of the first zero value

of the unit-radius aperture. When the subtraction rule is kept in mind it is clear that an annulus with these radii will now also give its first zero value in that direction.

The radius of the disk representing the heaviest atom should first be determined from considerations of the number of spectra which is to be rendered correctly, as explained above. This is then the unit radius. The radii of each ring representing a species of lighter atom in the structure with  $f$ -value a fraction of that of the heaviest atom can then be found by shifting the straight-edge parallel to itself until  $a_2^2 - a_1^2$  is the desired fraction. If, for instance, the light atom has half the scattering power of the heavy one, the values  $a_1 = 0.40$ ,  $a_2 = 0.81$  give the correct radii for the ring to represent the light atom. As  $0.81^2 - 0.40^2 = 0.5$ , the ring has half the area



Text-fig. 3. Amplitude at position of first zero value for unit-radius aperture plotted against radius of aperture,  $a$ , expressed as a fraction of that unit radius.

of the disk and hence gives a diffraction pattern with amplitude at the origin half that of the disk. The shape of the amplitude curve of this ring is also shown in Text-fig. 1. It has the same angular extent as the curve produced by the disk, but is everywhere approximately half the height.

If the object is to adjust conditions so that the amplitude curves of the apertures representing the different atoms fall away at different rates in order to simulate the varying rate of fall in  $f$  for light and heavy atoms, the size of the rings can be varied to give the first zero value at smaller angles.

When this scheme is used, a complication arises from the mechanism of the photographic development technique. We have hitherto assumed that we are dealing in the developed plate with perfectly transparent areas on a perfectly opaque background. In fact, however, in the developed photograph the transparent portions of the images of the rings are generally a good deal more dense than those of the large disks. Owing to scattered

light the grains of developed silver encroach on the transparent domains and obviously this effect is more serious for the rings. This should be allowed for by making the outside radius of the rings larger and the inside radius smaller than the calculated amount. The correction is necessarily empirical as it depends on the time of exposure and the development technique. To determine whether the correct amount of correction has been given the following preliminary experiment should be made:

The two apertures to be compared should be placed on the screen at the points  $(0, 0)$  and  $(0.5, 0.5)$  (or rather at  $(0.25, 0.25)$  and  $(0.75, 0.75)$  which avoid the cell corners) and a fly's eye photograph taken. The diffraction pattern produced by this grating has orders which are alternately strong and weak, as disturbances from the two sets of apertures are alternately in phase and out of phase. If, for instance, the aim is to get apertures representing two atoms one of which has half the scattering power of the other, the amplitudes of the sets of strong and weak orders should be in the ratio  $(1 + \frac{1}{2}) : (1 - \frac{1}{2})$ , that is 3:1, and the intensity ratio should therefore be 9:1. This case is illustrated in Plate 3, fig. 1.

#### Experimental details

*Making the multiple image photograph.* When the size of the disks and rings to represent the atoms has been chosen, they are placed at their co-ordinate positions on the illuminated background. This illuminated background, as explained by Stokes, should be made slightly larger than the correct size for the square unit cell in order to ensure that the background of the fly's eye photograph is black all over, and does not show slits of light where two adjacent pictures fail to unite because of an error in the position of the lenses.

An exposure is then made through the fly's eye plate on to the process plate, which after development forms the grating. In this connexion there are two points to be noted:

- (a) *Choice of origin.* When placing the disks on the illuminated screen it is best to try to choose the arbitrary origin in such a way that all disks avoid cell edges and corners. Placing a disk on an edge involves placing one on the opposite edge as well, and a disk on a corner needs similarly placed disks on the three other corners. The resultant aperture in the photograph is then built up by all these contributing disks, and any slight error in the position of a single lens will distort the shape of these composite images.
- (b) *Influence of exposure time.* As mentioned above the illuminated screen is slightly larger than the correct cell size. This causes the whole fly's eye photograph to be crossed by a square grid which has been given double the exposure of the background. Unless the total exposure is made so long that this grid is unnoticeable when the

picture is held up to a strong light, the spectra on the axes will be affected. The smaller the apertures used the more important this becomes. Plate 3, fig. 2 shows the diffraction pattern produced by this grid alone. The grating was obtained by putting no disk on the screen, and making the exposure time slightly too short.

A moderate overexposure followed by subtractive reduction with a strong solution of sodium thiosulphate to which a few drops of potassium ferricyanide solution have been added, is advantageous to brighten up the apertures, but this extra processing makes accurate control of the relative transmission of the differently sized apertures more difficult.

*Recording the diffraction images.* The diffraction pattern produced by the grating was obtained by using a mercury-vapour concentrated-source discharge lamp with a small pinhole aperture. The strong blue light of the source was isolated by using a deep blue filter. The grating, mounted with immersion oil between two optical flats, was placed between two lenses of about 150 cm. focal length. The first collimated the light from the source into a parallel beam, while the second produced the Fraunhofer diffraction pattern in its focal plane, where it was directly recorded on a fine grain plate. The orders of diffraction were separated only by about 0.5 mm. on this plate, but the use of a pinhole small compared with this separation, as well as very good-quality lenses, gave remarkably clear and well-resolved pictures. They could easily be studied by viewing with a reading lens against an illuminated sheet of paper.

*Estimation of intensity.* The intensity of the orders of diffraction was estimated by visually comparing the spots with an intensity scale. This intensity scale was made by photographing the image of the pinhole suitably reduced in intensity, and using the same lens system. A series of varying exposure times was given and the time-intensity reciprocity law was assumed to be valid in assigning intensity values to the graded row of spots. Using filters with known transmission coefficients a real intensity scale was also made, but visual comparison of the spots does not possess so high an accuracy that any significant difference could be detected between the time scale and the real intensity scale.

As the intensities of the different orders of diffraction vary by very large factors, one photograph of the diffraction pattern was generally not sufficient. Three photographs differing in exposure times by a factor of five were found to be adequate.

### Results

(a) *Sodium chloride.* The strong and weak X-ray reflexions of sodium chloride for orders with even and odd indices can be demonstrated by means of the fly's eye when the structure of NaCl projected on (110) is placed on the screen. The rings representing the sodium ions should have half the area of the solid disks which

represent the chlorine ions. As the repeat distances for this projection are in the ratio  $1 : 1/\sqrt{2}$ , the  $f$ -values for orders of reflexion along the two axes do not fall off at the same rate. To get this effect with the square screen of the fly's eye, ellipses and elliptical rings were used instead of circles. These ellipses had axes in the same ratio  $1 : 1/\sqrt{2}$ ; the major axis coincided with the short cell edge. Plate 3, fig. 3 shows the diffraction pattern obtained, with the strong spectra on the average nine times more intense than the weak spectra.

(b) *Iron pyrites.* As it was considered that the actual vanishing of certain orders might be a better test for the fly's eye, the  $h00$  orders of iron pyrites,  $\text{FeS}_2$ , were obtained. These spectra as measured on the ionization spectrometer have intensities 100, 0, 0, 14, 4 (Bragg, 1913). The vanishing of the second and third orders is due to the position of planes of sulphur atoms dividing the Fe-Fe distance in the ratio  $1 : 5$ .

When disks of the correct size for iron, together with half-area rings for the sulphur atoms, were placed on the screen at points having the correct  $x$  co-ordinates, the orders of diffraction given by the fly's eye grating along this axis had the intensities shown in Plate 3, fig. 4, which is in good agreement with the X-ray intensities.

(c) *Diopside.* When the unit cell of diopside (Warren & Bragg, 1928) is projected on the (010) plane it is very elongated in shape with cell edges in the ratio 1.85 : 1. Furthermore, the cell has an obtuse angle of  $105^\circ 50'$ . It was therefore a good test for the fly's eye apparatus to try to render the  $h0l$  reflexions correctly, especially as the structure contains atoms of widely different scattering factor.

The right *shape* and *orientation* for the ellipses to be used were found as explained above. The necessary axial ratio of the ellipses was found to be 2.05 : 1, and they had to be so oriented that their major axes made an angle of  $15^\circ$  with the  $z$ -axis of the square fly's eye cell (Plate 4, fig. 5). The correct *sizes* for the diffraction disks and rings were found in the following way: The  $f$ -values for the constituent atoms at small angles of reflexion are in the following ratio:

Ca + Mg (superimposed)	24.4
Si	10.2
O	6.6

The areas had therefore to be in this ratio, duly allowing for the photographic density effect. It was decided to render correctly the first five spectra along  $h$  and the first three along  $l$ . For the highest of these spectra the  $f$ -value for Ca + Mg has fallen to 0.4 of its low-angle value, for Si also to 0.4, and for O to 0.2. The sizes of the disks and rings were therefore calculated to give this same falling off in the single-aperture diffraction pattern at the positions where these optical orders occurred. This necessitated using quite large and narrow rings for the oxygen atoms, which had the unfortunate result that two overlapped as shown in Plate 4, fig. 5. However, the parts of the rings actually super-

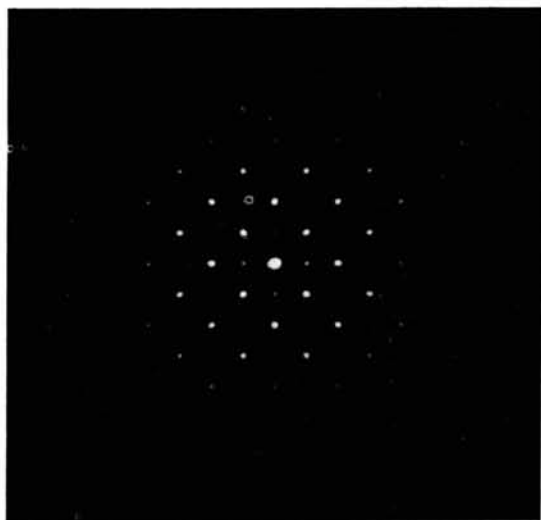


Fig. 1. Alternate strong and weak orders.

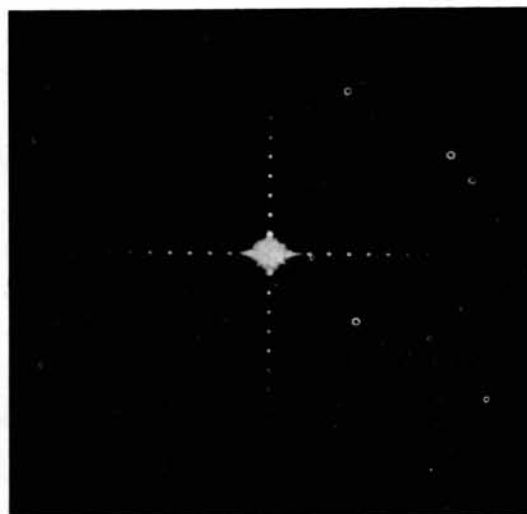


Fig. 2. Diffraction pattern produced by under-exposed fly's eye grating without any apertures.

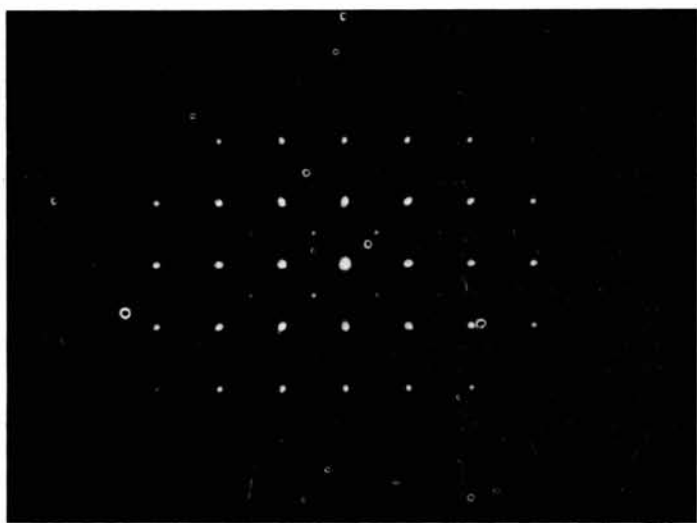


Fig. 3. The strong and weak orders produced by NaCl.

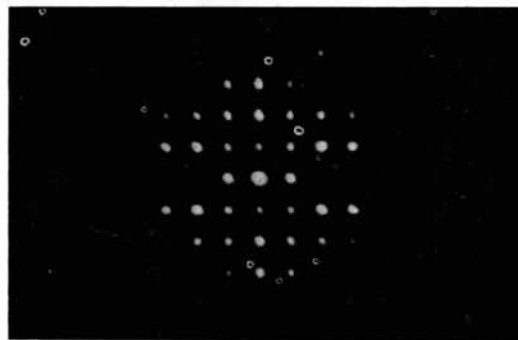


Fig. 4. The  $h00$  spectra of iron pyrites,  $\text{FeS}_2$ . Only orders along the horizontal axis are significant.

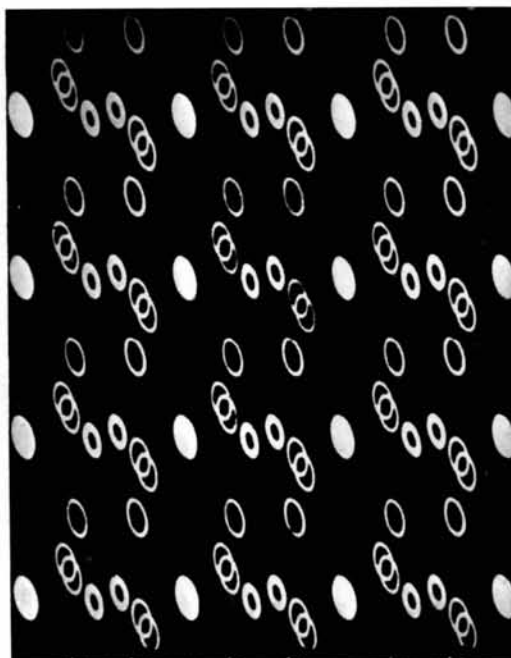


Fig. 5. Enlargement of a small part of the diopside grating.

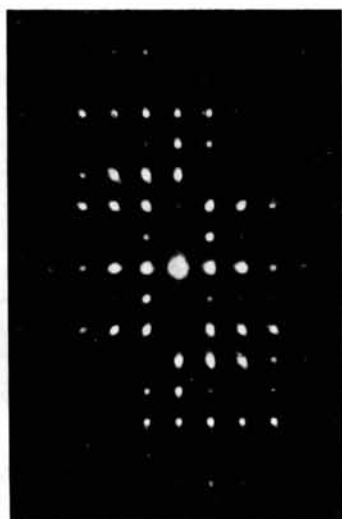


Fig. 6. Optical diffraction pattern of diopside grating with elliptical apertures.

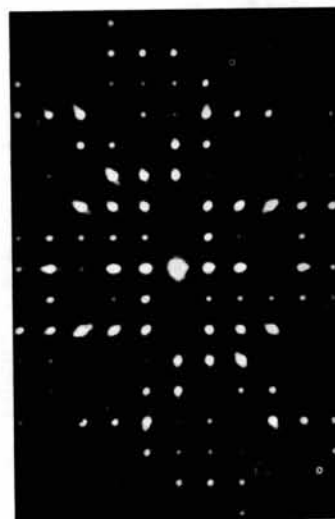


Fig. 7. Optical diffraction pattern of diopside grating with circular apertures.

imposed were small compared with their total area; consequently this overlapping did not have a serious effect.

The arbitrary origin on the illuminated screen was so chosen that no atom had to be duplicated in order to render the structure correctly. The repeating pattern in this projection is the quarter unit cell, thus only X-ray reflexions with even indices are present. It was therefore necessary to put only the contents of the quarter unit cell on the fly's eye screen. The indices of the optical orders of diffraction obtained were then doubled.

calculated intensities is good but not perfect. This must be due to the fact that there is only approximate similarity between the atomic *f*-curves and the single-aperture amplitude curves. The agreement is, however, so good that there is no difficulty in recognizing the substantial correctness of a proposed structure. Used as above the fly's eye apparatus can therefore be a valuable aid for the quick and approximate determination of intensities, not only when the atoms all have the same scattering factor, but also when both light and heavy atoms are present.

Table 1. Observed intensities of the orders of diffraction given by the diopside grating compared with the calculated intensities of the *h0l* X-ray reflexions

<i>h</i> \ <i>l</i>	$\bar{6}$		$\bar{4}$		$\bar{2}$		0		2		4		6	
	Obs.	Calc.	Obs.	Calc.	Obs.	Calc.	Obs.	Calc.	Obs.	Calc.	Obs.	Calc.	Obs.	Calc.
0	30	23	170	114	300	300	—	—	300	300	170	114	30	23
2	0	0	5	5	70	72	2	1	15	19	5	0	5	18
4	30	51	80	70	120	98	5	3	150	137	100	72	60	23
6	0	2	2	4	0	0	120	130	120	110	140	92	20	7
8	—	—	5	10	30	26	50	48	10	9	0	0	—	—
10	—	—	—	—	40	56	40	31	50	48	—	—	—	—

Plate 4, fig. 6 shows the optical diffraction pattern obtained, using this diopside grating. Table 1 compares the estimated relative intensities of the diffracted orders with the calculated intensities of the *h0l* reflexions of the diopside crystal. The arbitrary scale for the estimated intensities was adjusted to give equal values for 002.

Plate 4, fig. 7 shows the diffraction pattern obtained when circular disks of the correct areas are used instead of the elliptical disk and rings. It is clear that the intensities of Plate 4, fig. 6 show a much better agreement than Plate 4, fig. 7 with the calculated values.

It is seen that the agreement between observed and

I wish to thank Prof. Sir Lawrence Bragg who suggested the problem and who showed unfailing interest in its development, and Dr Helen Megaw for many helpful discussions and willing co-operation.

References

AIPER, G. B. (1834). *Trans. Camb. Phil. Soc.* **5**, 283.  
 BRAGG, W. L. (1913). *Proc. Roy. Soc. A*, **89**, 468.  
 BRAGG, W. L. (1944). *Nature, Lond.*, **154**, 69.  
 PRESTON, T. (1928). *Theory of Light*, 5th ed. London: Macmillan.  
 STOKES, A. R. (1946). *Proc. Phys. Soc., Lond.*, **58**, 306.  
 WARREN, B. E. & BRAGG, W. L. (1928). *Z. Kristallogr.* **69**, 168.